

**DRAG REDUCTION ON NACA 2412 USING
DIMPLED AIRFOIL AND GROOVED WING**

SAMUEL MERRYISHA SWEETY GRACIA

UNIVERSITI SAINS MALAYSIA

2020

**DRAG REDUCTION ON NACA 2412 USING
DIMPLED AIRFOIL AND GROOVED WING**

by

SAMUEL MERRYISHA SWEETY GRACIA

**Thesis submitted in fulfilment of the requirements
for the degree of
Master of Science**

July 2020

ACKNOWLEDGEMENT

Thanks and glory to Lord Jesus Christ, for his abundant showers of blessings, protection and strength for determination to pursue my study and make this research successful despite struggles and pains.

First and foremost, I would like to express my sincere gratitude and deepest appreciation to my supervisor, Associate Professor Ir. Dr. Parvathy Rajendran, who gave constant encouragement, support and guidance through all her experience and suggestions right from the very beginning. Time and efforts by her in all the midway of difficulties has boosted and enriched my research study. Her confidence in me and her positive personality gave me a great source of inspiration and motivation, which steer me to accomplish my research smoothly.

I want to extend my utmost gratitude to the Dean of School of Aerospace Engineering, Associate Professor Dr. Farzad Ismail, who has helped and encouraged me in all the stages of difficulties. I am particularly indebted to my former dean Professor Ir. Dr. Mohd Zulkfy Abdullah with sincere appreciation for his initial stage of application acceptance. I feel blessed to have a unique and outstanding educational experience in Universiti Sains Malaysia with a lot of amenities and caring souls around, which is much essential for my current academic and future professional growth.

Also, I want to dedicate my thankfulness to all the people who laid down as a stepping stone either directly or indirectly in all my aspires in Malaysia.

My sincere gratitude and extreme appreciation to USM for USM Fellowship, which has allowed me to focus more on my studies and project, once again, I thank you for your generous support.

Last but not least, special thanks to my parents Er. D Samuel & Er. Binola Samuel and my brother Mr. Divyesh Samuel for their selfless love, encouragement and moral support. I owe a debt of gratitude to my family for all their sacrifices and immeasurable contribution, which kept me stronger to mover further to fulfil all my goals.

TABLE OF CONTENTS

| | |
|---|-------------|
| ACKNOWLEDGEMENT | ii |
| TABLE OF CONTENTS | iv |
| LIST OF TABLES | vii |
| LIST OF FIGURES | ix |
| LIST OF SYMBOLS | xii |
| LIST OF ABBREVIATIONS | xiv |
| ABSTRAK | xv |
| ABSTRACT | xvii |
| CHAPTER 1 INTRODUCTION | 1 |
| 1.1 Overview | 1 |
| 1.2 Research background | 1 |
| 1.3 Problem statement | 7 |
| 1.4 Research objective and aim | 8 |
| 1.5 Scope of research | 8 |
| 1.6 Thesis organization | 9 |
| CHAPTER 2 LITERATURE REVIEW | 11 |
| 2.1 Overview | 11 |
| 2.2 Rough surface aerodynamics survey | 11 |
| 2.3 Golf ball concept | 12 |
| 2.3.1 Types of surface modifier and concept behind it | 13 |
| 2.3.2 Behaviour of attached flow and re-attached flow | 16 |
| 2.4 Dimple surface behaviour and its aerodynamic performance | 18 |
| 2.5 Grooved surface behaviour and its aerodynamic performance | 23 |
| 2.6 Summary | 27 |

| | | |
|------------------|--|-----------|
| CHAPTER 3 | METHODOLOGY | 30 |
| 3.1 | Overview | 30 |
| 3.2 | Design models | 32 |
| 3.2.1 | Dimple model | 32 |
| 3.2.2 | Groove model | 39 |
| 3.3 | Governing equation and mathematical formulation | 40 |
| 3.4 | Turbulence modelling | 42 |
| 3.5 | Numerical setup for computational fluid dynamic analysis | 44 |
| 3.5.1 | Computational domain and mesh generation | 44 |
| 3.5.2 | Boundary condition for both studies | 47 |
| 3.6 | Reliability and validation | 50 |
| 3.6.1 | Mesh independency study | 51 |
| 3.6.2 | Turbulence model independency study | 52 |
| CHAPTER 4 | RESULTS AND DISCUSSION | 55 |
| 4.1 | Overview | 55 |
| 4.2 | Modified airfoil study | 55 |
| 4.2.1 | Aerodynamic behaviour of dimple airfoil | 55 |
| 4.2.1(a) | Lift coefficient of airfoil models | 56 |
| 4.2.1(b) | Drag coefficient of airfoil models | 59 |
| 4.2.1(c) | Lift to drag ratio of airfoil models | 62 |
| 4.2.2 | Aerodynamic behaviour of dimple based on the location of chord | 65 |
| 4.2.2(a) | Dimple located at 30% of the airfoil chord | 65 |
| 4.2.2(b) | Dimple located at 50% of the airfoil chord | 67 |
| 4.2.2(c) | Dimples located at 70% of the airfoil chord | 68 |
| 4.2.2(d) | Dimples located at suction side of the airfoil chord | 70 |
| 4.2.2(e) | Dimples located at suction and pressure side of the airfoil | 71 |

| | | |
|--|---|------------|
| 4.2.3 | Performance of dimple airfoil models based on aerodynamic aspects | 74 |
| 4.2.3(a) | Lift coefficient of dimple airfoil models | 74 |
| 4.2.3(b) | Drag coefficient of dimple airfoil models | 77 |
| 4.2.3(c) | Lift to drag ratio of dimple airfoil models | 79 |
| 4.2.4 | Dimple airfoil output visualization | 81 |
| 4.3 | Groove wing study | 86 |
| 4.3.1 | Aerodynamic characteristics of groove wing | 86 |
| 4.3.1(a) | Lift coefficient of wing models | 86 |
| 4.3.1(b) | Drag coefficient of wing models | 87 |
| 4.3.1(c) | Lift to drag ratio of wing models | 88 |
| 4.3.2 | Low AR wing output visualization | 89 |
| 4.4 | Overall discussion | 92 |
| 4.4.1 | Overall discussion on dimple airfoil study | 92 |
| 4.4.2 | Overall discussion on modified low AR wing | 96 |
| CHAPTER 5 CONCLUSION & FUTURE WORKS | | 97 |
| 5.1 | Overview | 97 |
| 5.2 | Conclusion | 97 |
| 5.3 | Recommendation | 99 |
| REFERENCES | | 100 |
| LIST OF PUBLICATIONS | | |

LIST OF TABLES

| | Page |
|---|-------------|
| Table 2.1 Types of surface modifiers with performance categorization | 15 |
| Table 2.2 Existing dimple parameters | 21 |
| Table 2.3 Aerodynamic performance of different dimple shapes | 23 |
| Table 2.4 Existing groove parameters | 25 |
| Table 2.5 Best modifier parameters | 29 |
| Table 3.1 NACA 2412 Airfoil Model-1 Original airfoil (OA) | 33 |
| Table 3.2 Advantages/limitations of different turbulence model | 43 |
| Table 3.3 Boundary condition and specification | 49 |
| Table 3.4 Grid convergence study | 51 |
| Table 3.5 Average percentage of error at different turbulence models | 54 |
| Table 4.1 Percentage drop in lift by dimple models | 59 |
| Table 4.2 Percentage drop in drag of variable dimple location | 73 |
| Table 4.3 Percentage improvement in l/d of variable dimple location | 74 |
| Table 4.4 Performance of round dimple airfoil Models based on C_l | 75 |
| Table 4.5 Performance of square dimple airfoil Models based on lift coefficient | 75 |
| Table 4.6 Performance of rectangular dimple airfoil models based on C_l | 75 |
| Table 4.7 Performance of oval dimple airfoil models based on C_l | 76 |
| Table 4.8 Performance of hexagonal dimple airfoil models based on C_l | 76 |
| Table 4.9 Performance of round dimple airfoil models based on C_d | 77 |
| Table 4.10 Performance of square dimple airfoil models based on C_d | 78 |
| Table 4.11 Performance of rectangular dimple airfoil models based on C_d | 78 |
| Table 4.12 Performance of oval dimple airfoil models based on C_d | 78 |
| Table 4.13 Performance of hexagonal dimple airfoil models based on C_d | 79 |

| | |
|--|----|
| Table 4.14 Performance of round dimple airfoil models based on C_l/C_d | 80 |
| Table 4.15 Performance of square dimple airfoil models based on C_l/C_d | 80 |
| Table 4.16 Performance of rectangular dimple airfoil models based on C_l/C_d | 80 |
| Table 4.17 Performance of oval dimple airfoil models based on C_l/C_d | 81 |
| Table 4.18 Performance of hexagonal dimple airfoil models based on C_l/C_d | 81 |
| Table 4.19 2-d airfoil Pressure contour | 82 |
| Table 4.20 2-d airfoil Velocity contour | 82 |
| Table 4.21 2-d airfoil Stream line pattern | 84 |
| Table 4.22 2-d airfoil Flow rendering | 85 |
| Table 4.23 Percentage improvement in lift to drag ratio | 88 |
| Table 4.24 Dimple Airfoil model individual performance | 94 |

LIST OF FIGURES

| | Page |
|--|-------------|
| Figure 1.1 Airfoil boundary layer flow behaviour | 2 |
| Figure 1.2 Turbulence re-attachment | 3 |
| Figure 1.3 Golf ball flow behaviour | 4 |
| Figure 1.4 Flow control techniques | 5 |
| Figure 1.5 Existing wing surface modifiers | 7 |
| Figure 2.1 Golf ball specification | 13 |
| Figure 2.2 Airfoil nomenclature | 16 |
| Figure 2.3 Diffusion of flow within the cavity | 19 |
| Figure 2.4 Ribs over wing mounted inside wind tunnel | 26 |
| Figure 3.1 Methodology | 31 |
| Figure 3.2 Indented dimple models | 35 |
| Figure 3.3 Protruded dimple models | 38 |
| Figure 3.4 Different groove models | 39 |
| Figure 3.5 Groove dimensions (dimensions are in mm) | 40 |
| Figure 3.6 CFD processing stages | 44 |
| Figure 3.7 Projected view of domain with airfoil in the mist | 45 |
| Figure 3.8 Isometric view of a semi-bullet domain | 45 |
| Figure 3.9 2D domain grid generation | 46 |
| Figure 3.10 Dimple fine refined mesh | 46 |
| Figure 3.11 Fine grid wing | 47 |
| Figure 3.12 Solver setup | 48 |
| Figure 3.13 Workflow in validation | 50 |
| Figure 3.14 Groove wing with standard meshing | 52 |

| | |
|---|----|
| Figure 3.15 Groove wing with coarse meshing | 52 |
| Figure 3.16 Groove wing with medium meshing | 52 |
| Figure 3.17 Groove wing with fine meshing | 52 |
| Figure 3.18 C_l vs AOA for different turbulence models | 53 |
| Figure 4.1 C_l vs AOA of Round dimple airfoil compared to original airfoil | 56 |
| Figure 4.2 C_l vs AOA of square dimple airfoil and original airfoil | 57 |
| Figure 4.3 C_l vs AOA of rectangular dimple airfoil and original airfoil | 57 |
| Figure 4.4 C_l vs AOA of oval dimple airfoil and original airfoil | 58 |
| Figure 4.5 C_l vs AOA of hexagonal dimple airfoil and original airfoil | 58 |
| Figure 4.6 C_d vs AOA of round dimple airfoil and original airfoil | 59 |
| Figure 4.7 C_d vs AOA of square dimple airfoil and original airfoil | 60 |
| Figure 4.8 C_d vs AOA of rectangular dimple airfoil and original airfoil | 60 |
| Figure 4.9 C_d vs AOA of oval dimple airfoil and original airfoil | 61 |
| Figure 4.10 C_d vs AOA of hexagonal dimple airfoil and original airfoil | 61 |
| Figure 4.11 C_l/C_d vs AOA of round dimple airfoil and original airfoil | 62 |
| Figure 4.12 C_l/C_d vs AOA of square dimple airfoil and original airfoil | 63 |
| Figure 4.13 C_l/C_d vs AOA of rectangular dimple airfoil and original airfoil | 63 |
| Figure 4.14 C_l/C_d vs AOA of oval dimple airfoil and original airfoil | 64 |
| Figure 4.15 C_l/C_d vs AOA of hexagonal dimple airfoil and original airfoil | 64 |
| Figure 4.16 C_l vs AOA of dimples located at 0.3C airfoil | 65 |
| Figure 4.17 C_d vs AOA of dimples located at 0.3C airfoil | 66 |
| Figure 4.18 C_l/C_d vs AOA of dimples located at 0.3C airfoil | 66 |
| Figure 4.19 C_l vs AOA of dimples located at 0.5C airfoil | 67 |
| Figure 4.20 C_d vs AOA of dimples located at 0.5C airfoil | 67 |
| Figure 4.21 C_l/C_d vs AOA of dimples located at 0.5C airfoil | 68 |
| Figure 4.22 C_l vs AOA of dimples located at 0.7C airfoil | 68 |

| | |
|---|----|
| Figure 4.23 C_d vs AOA of dimples located at 0.7C airfoil | 69 |
| Figure 4.24 C_l/C_d vs AOA of dimples located at 0.7C airfoil | 69 |
| Figure 4.25 C_l vs AOA of dimples located at suction side of airfoil | 70 |
| Figure 4.26 C_d vs AOA of dimples located at suction side of airfoil | 70 |
| Figure 4.27 C_l/C_d vs AOA of dimples located at suction side of airfoil | 71 |
| Figure 4.28 C_l vs AOA of dimples located at suction & pressure side of airfoil | 71 |
| Figure 4.29 C_d vs AOA of dimples located at suction & pressure side of airfoil | 72 |
| Figure 4.30 C_l/C_d vs AOA of dimples located at suction & pressure side of airfoil | 72 |
| Figure 4.31 C_L vs AOA of various groove configuration wing models | 86 |
| Figure 4.32 C_D vs AOA of various groove configuration wing models | 87 |
| Figure 4.33 Pressure distribution of low AR wing models at 16° AOA | 89 |
| Figure 4.34 Velocity distribution of low AR wing models at 16° AOA | 90 |
| Figure 4.35 Vortex flow visualization of different models | 91 |
| Figure 4.36 Stalling characteristics | 92 |
| Figure 4.37 Comparison of flow separation point of dimple model airfoil vs OA | 93 |

LIST OF SYMBOLS

ROMAN SYMBOLS

| | |
|-----------------|--|
| b | Distance between two dimples (mm) |
| c | Dimple diameter (mm) |
| C | Chord (mm) |
| C_l | Co-efficient of lift (2-dimensional) |
| C_L | Co-efficient of lift (3-dimensional) |
| C_d | Co-efficient of drag (2-dimensional) |
| C_D | Co-efficient of drag (3-dimensional) |
| d | Diameter (mm) |
| G_v | Turbulent viscosity (Kg/ms) |
| h | Depth of modifier (mm) |
| k | Dimple depth (mm) |
| $k-\omega$ | Turbulent model |
| $k-\varepsilon$ | Turbulent model |
| L | Length (mm) |
| L/D | Lift to drag ratio |
| Re | Reynolds number |
| s | Span (mm) |
| $S_{\bar{\nu}}$ | User-defined source term |
| u | Velocity (m/s) |
| u_τ | Shear velocity (m/s) |
| $u_i u_j$ | Mean velocity components |
| v | Velocity (m/s) |
| ν | Kinetic viscosity (m ² /s) |
| $\bar{\nu}$ | Modified turbulent viscosity (m ² /s) |

| | |
|--------|------------------------------------|
| x, y | Physical Cartesian coordinate axes |
| Y_v | Destruction of turbulent viscosity |
| Y^+ | Dimensionless wall distance |

GREEK SYMBOLS

| | |
|------------|---------------------------------------|
| Γ | Circulation |
| ∂ | Partial derivative |
| δ | Boundary layer thickness (m) |
| δ^* | Displacement thickness (m) |
| τ_w | Wall shear stress (N/m ²) |
| ρ | Fluid density (kg/m ³) |
| μ | Dynamic viscosity coefficient |

SUBSCRIPTS

| | |
|---|----------------------|
| D | Drag (3-dimensional) |
| d | Drag (2-dimensional) |
| L | Lift (3-dimensional) |
| l | Lift (2-dimensional) |

SUPERSCRIPTS

| | |
|---|--------|
| 2 | Square |
| o | Degree |

LIST OF ABBREVIATIONS

| | |
|--------------------|---|
| 2D | Two dimensional |
| 3D | Three dimensional |
| AOA | Angle of attack |
| AR | Aspect ratio |
| CFD | Computational fluid dynamics |
| DES | Detached Eddy Simulation |
| KE | Kinetic energy |
| LE | Leading edge |
| LED | Large Eddy Simulation |
| NACA | National Advisory Committee for Aeronautics |
| NASA | National Aeronautics and Space Administration |
| OA | Original Airfoil |
| RANS | Reynolds Averaged Navier Stokes |
| SA | Spalart Allmaras |
| SHD | Single Hexagonal Dimple |
| SOD | Single Oval Dimple |
| SPHD | Suction and Pressure side Hexagonal Dimple |
| SPOD | Suction and Pressure side Oval Dimple |
| SPRD | Suction and Pressure side Round Dimple |
| SPR _c D | Suction and Pressure side Rectangular Dimple |
| SPSD | Suction and Pressure side Square Dimple |
| SRD | Single Round Dimple |
| SR _c D | Single Rectangular Dimple |
| SSHD | Suction Side Hexagonal dimple |
| SSOD | Suction Side Oval Dimple |
| SSRD | Suction Side Round Dimple |
| SSR _c D | Suction Side Rectangular Dimple |
| SSD | Single Square Dimple |
| SSSD | Suction Side Square Dimple |
| TE | Trailing edge |
| VG | Vortex generator |

**PENGURANGAN SERET PADA NACA 2412 MENGGUNAKAN
AEROFIL BERLEKUK DAN SAYAP BERALUR**

ABSTRAK

Daya saing sayap berprestasi tinggi dengan ciri kepegunan yang lebih baik menjadi lebih popular dalam beberapa dekad kebelakangan ini. Faktor utama yang mendominasi kekurangan prestasi aerodinamik adalah pembentukan seretan. Aerodinamik permukaan kasar adalah salah satu kaedah alternatif yang menjanjikan penurunan seretan dan meningkatkan L/D dengan melibatkan teknik kawalan pasif. Dalam kajian semasa, interaksi parameter lesung dan alur yang mempengaruhi prestasi aerodinamik udara dan sayap pada sudut serangan yang berbeza yang beroperasi pada 30 m / s dan bilangan Reynolds 4.4×10^5 dipertimbangkan. Kajian ini terbahagi kepada dua, Kajian (1) meneroka prestasi dan tingkah laku aerodinamik dari lima lesung lekukan dan berlindung yang berlainan yang terletak di 1) 0.3C, 2) 0.5C, 3) 0.7C, 4) pelbagai lesung di bahagian sedutan sahaja dan 5) pelbagai lesung lekukan di seluruh pelantar udara (iaitu kedua-dua sisi tekanan dan penyedut) di atas 2D airfoil. Kajian (2) berkaitan dengan lekukan lekukan di bahagian sayap di lokasi x / c yang berbeza 1) dekat pinggir hadapan (0.2C), 2) dekat tepi belakang (0.8C), 3) jarak tengah (0.5C), 4) triplet lokasi (0.2C, 0.5C, 0.8C). Mengubah permukaan airfoil / sayap meningkatkan kekekapannya, dengan demikian menebalkan aliran yang dipasang kembali; oleh itu aliran tetap terpasang walaupun pada AOA yang lebih tinggi. Model yang dirancang menggunakan CATIA V5R20 dan ANSYS Fluent membantu mensimulasikan tingkah laku aliran, dan perbezaan prestasi aerodinamik antara model. Hasil kajian (1) menunjukkan memperkenalkan lesung arus udara tetap yang melekat melebihi 0.25C bahkan pada 16° AOA dengan (l/d) maksimum 39.5% peningkatan. Hasil kajian (2)

menunjukkan bahawa kehadiran alur meningkatkan ciri penghentian dengan menjaga aliran melekat hingga 18° AOA. Dalam semua model sayap berlekuk, L/D menunjukkan peningkatan sekurang-kurangnya 0.5% berbanding dengan sayap garis dasar. Walau bagaimanapun, ciri-ciri aerodinamik menunjukkan hasil yang jelas pada model SRD (I) 0.5, SOD (P) 0.3, SSRD (I), SSSD (I) dan SSSD (P) dalam kes kajian lipatan udara malap dan sayap triplet alur di kes kajian sayap alur. Analisis dari sayap udara dan sayap alur yang berlipat dengan konfigurasi yang berbeza menunjukkan kepekaan aliran ke atas aliran udara yang kasar pada sisi tekanan dan penyedut.

DRAG REDUCTION ON NACA 2412 USING DIMPLED AIRFOIL AND GROOVED WING

ABSTRACT

The competitiveness of high-performance wing with improved stalling characteristics gains more popularity in recent decades. The primary factor dominating the lack in aerodynamic performance is drag formation. Rough surface aerodynamics is one of the promising alternative method which involves passive control technique to degrade drag and improve lift to drag ratio. In current study, the interaction of dimple and groove parameters influencing the aerodynamic performance of airfoil and wing at a different angle of attack operating at 30 m/s and Reynolds number of 4.4×10^5 are considered. The present study divides into two, Study (1) explores the aerodynamic performance and behaviour of five different indented and protruded dimples located at 1) 0.3C, 2) 0.5C, 3) 0.7C, 4) multiple dimples on suction side alone and 5) multiple dimples indenting throughout airfoil (i.e. both pressure and suction side) over 2D airfoil. Study (2) deals with grooves indented over the wingspan at different x/c location 1) near leading edge (0.2C), 2) near trailing edge (0.8C), 3) mid-span (0.5C), 4) triplet location (0.2C, 0.5C, 0.8C). Altering the surface of airfoil/wing boosts its efficiency, thereby thickens the reattached flow; hence the flow is kept attached even at higher AOA. The models are designed using CATIA V5R20 and ANSYS Fluent helps to simulate the flow behaviour, and aerodynamic performance difference between models. The results of study (1) show introducing dimples over airfoil keep flow attached beyond 0.25C even at 16° AOA with $(l/d)_{\max}$ of 39.5% enhancement. The results of the study (2) show that the presence of grooves enhances the stalling characteristics by keeping the flow attached up to 18° AOA. In all the grooved wing

model, the L/D shows at least 0.05% improvement compared to baseline wing. However, the aerodynamic characteristics show the pronounced result on SRD(I) 0.5, SOD(P) 0.3, SSRD(I), SSSD(I) and SSSD(P) models in the case of dimple airfoil study and triplet groove wing in the case of groove wing study. The analyses of the dimpled airfoil and groove wing with different configurations showcased the sensitivity of flow over rough airfoil on pressure and suction side.

CHAPTER 1

INTRODUCTION

1.1 Overview

The concept of motivation on wing surface optimization, flow behaviour, including the dimple and groove surfaces, are introduced in this chapter. In addition, research background, problem statement, research objectives, aim and scope of research are discussed in detail in this chapter.

1.2 Research background

Aerodynamics, the concept of studying the interaction of air on the moving bodies, which laid-down as the backbone to design various airborne vehicles. A vast improvement is in progress towards the low-speed flight to sustain the “off-design condition”, relative attentions are given to optimized airfoil to beat the complex high-speed to lift devices (McMasters and Henderson, 1979).

The predominate forces acting on the aircraft' are lift, drag, thrust and weight. All these forces play out a vital role in aircraft during flight, where the maximum lift is generated by aircraft wing. These wings are streamlined body (airfoil) which has a higher capability to generate more lift and minimal drag compared to the bluff body. The generation of lift is mainly due to the pressure difference on the suction and pressure side of the wing. Hence, importance has to be given in designing a wing to improve the aerodynamic performance.

There seems to be a drastic development in aircraft design comparative to past decades, in the sector of aerodynamic performance enhancement. Over decades scientist are very curious towards the optimized lift generation designs, in order to

enhance the aircraft characteristics. Significant efforts have shown up in degrading the surface shear stress, which affects the boundary layer. Thus, challenges have to be faced to improve the satisfactory performance of lift incorporated with minimal drag formation and delayed flow separation, particularly at a higher angle of attack (AOA).

The physical flow behaviour around an airfoil throws out a better understanding of engineering disciplines of existing aerodynamic design and encourages a leap to improve surface argumentation. When an object pear through fluid, a boundary layer is enclosed around the object, which further guides its performance. When the flow gets initialized, the flow maintained to be laminar as long as the surface is smooth, this will eventually lead to layer separation (Mahesh Babu et al., 2015, Groh, 2016) (as shown in Figure 1.1). This flow separation is mainly due to non-linear breakdown of flow over the smooth surface, generating shear layer which decays the aerodynamic performance (Ghazali et al., 2016, Guha et al., 2013). Hence, importance has to be shown in governing the laminar and turbulence flow.

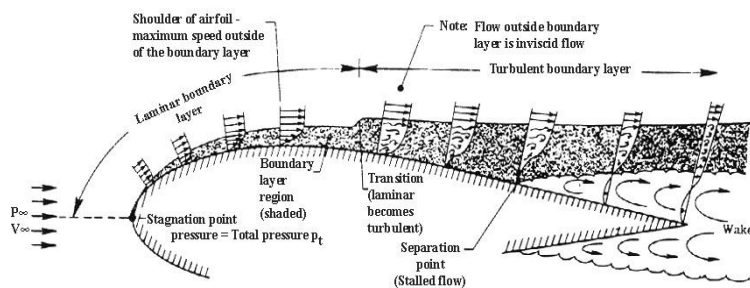


Figure 1.1 Airfoil boundary layer flow behaviour (Groh, 2016)

By inserting turbulence through the shear layer (as shown in Figure 1.2), the detached flow re-attaches the surface due to its natural adhesive property (Mahesh Babu et al., 2015, Shan et al., 2008, Choudhry et al., 2015). Researchers have showcased that the early detachment of flow is the primary reason for the hike in drag

and drop in lift. There is a considerable variant of issues hinders the airborne vehicles (aircrafts) performance; one among them is stalling factor. Hence, different active and passive modifiers are embossed on the wing surface, which disturbs the boundary layer flow and thus results in attached flow incorporated with streamwise vorticity.

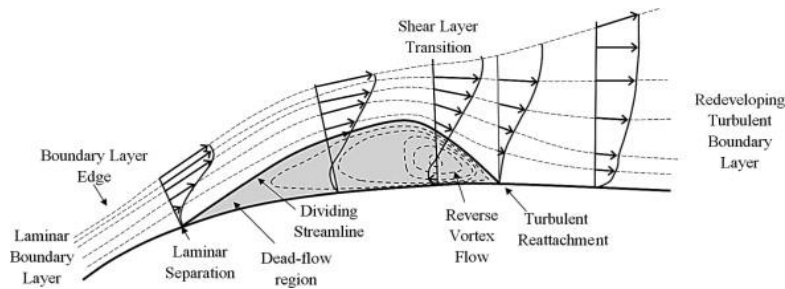


Figure 1.2 Turbulence re-attachment (Choudhry et al., 2015)

These surface modifiers act as a flow deflector. At stall condition the lift drops and drag heaps (i.e.) at higher AOA region. Further, the percentage drop of lift increases at critical AOA, where they undergo dominant flow separation. Thus, these flow separation lags the lift generated by the wing.

The latest era towards improving the fuel economy is through rough surface aerodynamics commonly via wing surface modifiers to increase the angle of the stall and decrease pressure drag by delaying the boundary layer separation. Improved aerodynamic efficiency enhances the commercial and military use of air vehicles. Hence, creating roughness on to the surface of the wing has attracted the attention of researchers in the recent trend (Guha et al., 2013).

Since the late 1800s, scientist commenced to analyse the rough surface aerodynamics. The first famous rough surface study was by Taylor (1908), by using dimples on a golf ball. These dimples proved to show the translation of transition point

towards the edge of the golf ball by cut-shortening the laminar flow boundary layer (Miller, 2012) (as shown in Figure 1.3).

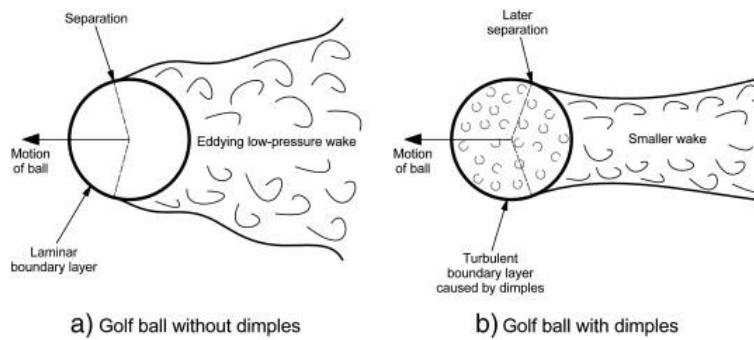


Figure 1.3 Golf ball flow behaviour (Bearman and Harvey, 1976, Miller, 2012)

Benefits were observed by reducing the pressure drag, though the skin friction drag showed slight increase due to the presence of rough surface. Followed by the in-depth survey was done by Harvey and Bearman (Bearman and Harvey, 1976), their excellent intense survey showed that the drag formation of a golf ball was higher compared to the smooth ball until the post-critical Reynolds number (Re_c). The dimples on the golf ball create smaller wakes behind the ball, resulting in total drag reduction with a smaller vortex zone.

The total drag mainly focuses on induced drag and frictional drag. Frictional drag heaps due to the boundary separation and it is dependent on Re_c . Studies show (Viswanath, 2002) frictional drag covers 40 – 50% of total drag at higher AOA. Thus, the concept of using Indented surface is implemented as it decreases frictional drag along with the creation of the laminar-turbulent transition layer. This golf ball generates more extended range and trajectory with massive resistance of airflow around the dimpled surface compared to the smooth surface.

Engineers employed these ideas on flying vehicles and hence variant of surface protrusions and depressions were designed (Kapoor and Jaykrishnan, 2018, Livya et al., 2015). Separation control or decay shows a vast improvement in the performance of airfoil/wing (Saravi and Cheng, 2013, Mahesh Babu et al., 2015). Recent competitive flow control techniques (as shown in Figure 1.4) (Ganesh et al., 2019, Yousefi and Saleh, 2015, Stanewsky, 2001) are: 1) Active modifiers: process involves improving the aerodynamic characteristics by generating additional kinetic energy (K.E) to the flow-through blowing or suction process, by retrofitting control devices over surface, 2) Passive modifier: modifying the wing surface to disturb the pressure distribution, thereby delays/ prevents the flow separation.

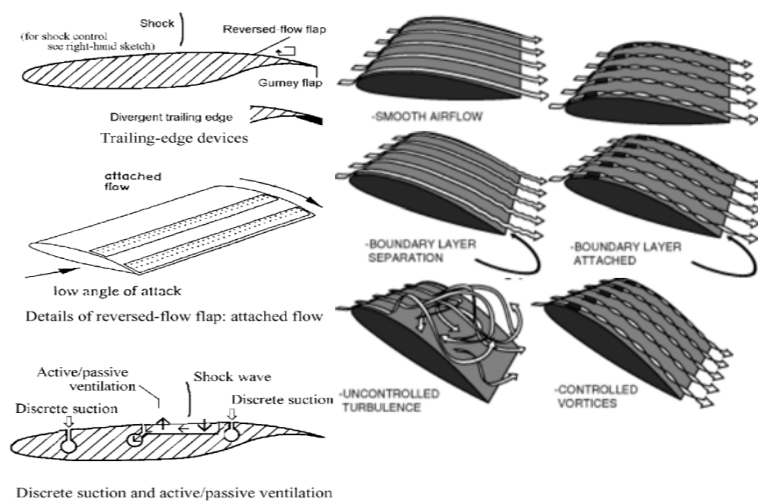


Figure 1.4 Flow control techniques (Stanewsky, 2001)

This flow control devices influence the boundary flow by redirecting the flow field; hence the adverse interaction of the flows is interrupted. Delaying the flow separation improves the maximum cross-sectional load with cutting down aerodynamic drag (Mariotti et al., 2018). In order to improve the manoeuvrability of

the aircraft, various surface modifiers are developed and also some are under research. Indentation over a smooth surface fosters the smooth flow by re-circulating it. These re-circulated flows pull back the separated flow to be attached for a more extended period of time.

Vortex generators (VG) initially plays out the vital role in controlling the flow separation at the range of subsonic condition. VG's are active or passive vanes over the wing surface, which alters the angle of stall by providing extra momentum (or) energy to the boundary layer and thereby delays the flow separation (Jumahadi et al., 2018, Seshagiri et al., 2009).

In this study, one such attempt has been enhanced to increase the aerodynamic efficiency by creating dimples over airfoil and grooves over wing surface. The ideology of the dimple effect on the wing/airfoil surface has been inspired by golf ball dynamics. Dimple/groove generates streamwise vortices by manipulating the flow behaviour. These streamwise vortices energize the flow momentum near the wall.

The general existing surface modifiers which are designed and analysed both numerically and experimentally by the researches are classified in Figure 1.5. These modifiers are typically round, square (or) triangular, which are higher than boundary layers, run through the wing surface along the spanwise direction (Baweja et al., 2016). All these different types of modifiers differ in their performance based upon their orientation and flow properties.

The complete effectiveness study is based on depth, shape, size and orientation of the modifier, also importance should be given to the corners of the modifiers. These parameters changes the turbulence effect of the flow (Devi and Shah, 2016) along with shifting of adverse pressure gradient.

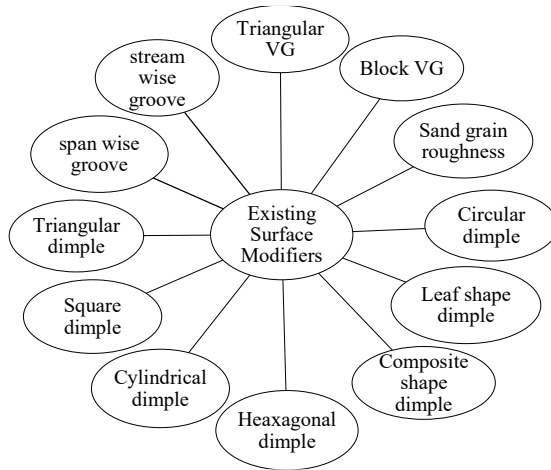


Figure 1.5 Existing wing surface modifiers (D'Alessandro et al., 2019, Seo and Hong, 2016, Taylor, 1947, Mahesh Babu et al., 2015)

1.3 Problem statement

The boundary layer manipulation (i.e. separation and stalling) and drag formation are the critical phenomenon to improve aerodynamic performance for external wall bounded flows. Dynamic stall vortex is one such phenomenon which arises during higher AOA, generating higher suction near the LE, thereby improves flow separation and rapid drag formation (Gupta and Ansell, 2018). In order to minimize the intensity of separation, these slowing down layers has to be “energized” and “accelerated”. The boundary layer flow can be energized through implementing roughness over the smooth surface thereby can delay stalling. When early flow separation takes place airfoil/wing experiences drop in lift and increase in drag formation.

The attention towards dimples and grooves have not shown up much importance as compared to VG's. Earlier VG's are the common passive modifiers, which energizes the upcoming flow by transiting laminar flow to turbulent and recent interest are towards dimples due to golf ball improved flow behaviour. The performance of dimples and grooves varies with size, shape and location.

Therefore, the present work focuses on the enhancement of airfoil/wing efficiency by creating dimples and grooves with variable size, shape and location. The goal is to postpone the stalling characteristics and decay drag formation with minimal surface changes.

1.4 Research objective and aim

- To introduce better airfoil model to improve drag reduction.
- To introduce better wing model to improve drag reduction.
- To investigate and differentiate the influence and aerodynamic performance of 10 different dimple models and semi-circular groove based on its chord location over aircraft airfoil and wing.

The aim of the research is as follows:

- Prolong or delay flow separation.
- Enhance the stalling angle.
- Reduced drag co-efficient.

1.5 Scope of research

The scope of the study is to analyse the aerodynamic flow behaviour using ANSYS FLUENT to simulate the process and to investigate the better adaptive dimple

shape and location. The study is based on different dimple and groove over NACA 2412 airfoil/wing. The airfoil models are studied at various AOA ranging from 0° to 22° at a constant velocity of 30 m/s.

Summary of project scope:

- NACA 2412 airfoil model is used.
- The domain extends 10 times the chord both horizontally and vertically around the model.
- Two sets of dimple models are designed 1) indented dimple, 2) protruded dimple using spherical, square, rectangular, oval and hexagonal shapes.
- Size and depth of the dimples are maintained to be constant.
- Indented semi-circular grooves are used in the case of wing study.

1.6 Thesis organization

The complete study is based on the impact of the roughness geometries (dimple & groove) over airfoil/wing on various flow regime using CFD numerical simulation. For documentation criterion, the thesis is broken into five chapters. Chapter 1 has covered the general introduction, research problems, along with a framework of the scope and objectives of this study. It also presents the research background motivation of this study, including the drawbacks of surface modifiers. The overall objective, aim, corresponding investigation techniques, along with the scope of research, is also discussed in this chapter.

Chapter 2 encompasses the literature review, which showcases research background with recent research and history of dimple formation and its aerodynamic properties. This chapter also focuses on the comparative behaviour of smooth vs rough

airfoil in the presence of alternative factors. At last, the chapter concludes with a beneficial literature review gap summary.

Chapter 3 is the methodology, which covers the present study involving design, analysis and validation, which mainly concentrates on numerical setup and procedures. This chapter introduces different dimple and groove models.

Chapter 4 brings out the impact of dimple/groove behaviour on the laminar boundary layer separation point and analyse the numerical results obtained from CFD simulation. These results are compared and discussed with the validation data to determine the aerodynamic performance variation.

Chapter 5 draws the overall significant-conclusion observed from this research and suggest paths of future investigation, which can be carried out.

CHAPTER 2

LITERATURE REVIEW

2.1 Overview

The pre-research contribution of various researchers is reviewed and discussed thoroughly in this chapter to determine the key characteristic contribution of various surface modifiers. It includes both experimental and numerical study. The chapter focuses on the essential aspects of aerodynamic improvement, which is in constant development. The literature survey concentrates on surface roughness, surface modifiers, dimples and grooves design. Thus, this chapter is purely based on passive surface modifiers.

2.2 Rough surface aerodynamics survey

The predominant factors which dominate the aircraft performance are lift and drag. Drag co-efficient plays a significant role for improving the aerodynamic aspects, which depends on 1) relative surface roughness, 2) AOA, 3) relative flow velocity, 4) shape, size and height, 5) fluid properties and 6) orientation of flow.

Surface modifiers generate streamwise vortex, which get re-circulated and mixes up with the wall-mounted flow. Hence, the mean velocity near the wall get increased with average momentum distribution, with a gain in momentum on the boundary layer velocity profile. The boundary layer mixing by this roughness over the surface makes the flow stabilized with delayed flow separation, with the early transition of laminar to turbulent.

In order to improve the airfoil/wing performance, dimples and grooves are distributed over the airfoil/wing with various orientation. Here, the background study has been concentrated more on variable dimple characteristics and its flow regime. The efficiency of dimple/groove characteristics has been extracted from previous literature for its optimum usage.

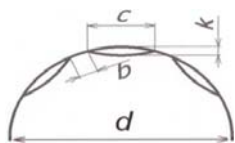
2.3 Golf ball concept

The golf ball concept had served out the outstanding performance in all aerodynamic sectors with the concept of golf ball dynamics, which has its era since the 1800s. Frictionless ball (smooth ball) showed up symmetrical pressure distribution, thereby generated massive wake formation with a drastic increase in drag (Ting, 2003). The wake formation opposes the forward movement of the ball with minimal lift. The dimples over the golf ball trip the air particles within it and rupture the smooth flow by recirculating the flow. These re-circulated flows energize the flow by creating linear momentum, which thereby keeps the flow to be attached for a longer period.

By creating a dimpling effect over a smooth ball shifts the critical region to lower Re with 50% cut down in drag co-efficient (Choi et al., 2006). As in the case of golf ball study (Bearman and Harvey, 1976), hexagonal dimple showed up the better performance in the case of aerodynamic efficiency at higher trajectory compared to round dimples. Hence, creating dimple influences the flow by energizing it.

The flight trajectory of the golf ball is influenced by the shape and size of the dimples and its purely aerodynamics. The effect of drag co-efficient at critical Re completely depends on the dimple size, shape, location and depth (Choi et al., 2006)

as shown in Figure 2.1. The dimple characteristics over a golf ball are studied in two different ways (Chowdhury et al., 2016, Choi et al., 2006), 1) Dimple depth ratio (Choi et al., 2006) and 2) Relative roughness (ϵ).



Where,
 d – golf ball diameter
 c – dimple diameter
 k – dimple depth
 b – distance between two dimples

Figure 2.1 Golf ball specification (Ting, 2003)

Studies revealed that shallow dimples over the golf ball decrease drag coefficient with a simultaneously reducing the lift generation for low-velocity condition (i.e.) below 30 m/s. Increasing the dimple size improves drag performance up to the limit Relative roughness, $c/d = 0.08$ and Dimple depth ratio, $k/d = 0.003$ (Naruo and Mizota, 2014, Ting, 2003, Aoki et al., 2009).

Detail study of golf ball dimpling effect (Chowdhury et al., 2016, Choi et al., 2006) shows that increasing the dimple depth results in shifting the critical region to lower Re with minimal drag formation, for instance, Dimple depth ratio of 0.4×10^{-2} which shifts the critical Re to 0.9×10^5 . Hence, shallow and deeper dimples have its range of performance based on the flight trajectory and flow re-circulation.

2.3.1 Types of surface modifier and concept behind it

Creating rough surface over an airfoil triggers the boundary layer with the interaction of turbulent flow by generating more kinetic energy and linear momentum to the flow, thereby minimise the drag formation (Choi et al., 2006). Every design parameters of the protrusion (or) depression on the wing surface has its cores of benefits towards compressible and incompressible flow.

The impact of co-efficient of drag (C_D) varies with dimension of the surface modifiers. According to Harun Chowdhury (Chowdhury et al., 2016), each dimension of the modifiers could change the transition region and C_D at trans-critical regime to lower Re . Hence, the performance of the wing is very sensitive to the wing surface. During higher AOA, the VG's acts as a vane on the suction side of the wing, which fosters the momentum transfer and keeps the flow re-attached due to co-rotated flow; these reattachments occurs at the downstream of the modifier.

The key concept behind is that the trailing vortices are generated streamwise along with the fluid flow, which thereby increases the transfer of momentum. The constant streamwise flow approach incorporated with the relationship between the velocity (v) and circulation (Γ) are studied (Isaacs, 1945). Thus, VG's are found to be the boundary layer energizer by mixing high energy free stream fluid (Seshagiri et al., 2009, Agarwal and Kumar, 2016, Neittaanmäki et al., 2004).

Some of the prominent findings on surface modifiers are tabulated below in Table 2.1. Majority of the research work says; the inward dimple performs better compared to the outward dimple in delaying the stalling characteristics (Hossain et al., 2015, Ramprasad and Devanandh, 2015).

Roughness height, spacing and skewness are the critical parameters considered in sand grain roughness modifier. Analysis results show that the turbulence intensity visualizes to be more massive behind the TE, which could be altered with uniform or random sand grain distribution (Ali et al., 2017). Inward and outward dimples have a variable performance for the same flow condition and AOA.

Table 2.1 Types of surface modifiers with performance categorization

| No. | Author | Type of modifiers | Airfoil | Method | Flow behaviour | Model | Description |
|-----|-------------------------------|--------------------|--------------|--------------|----------------|---------|--|
| 1. | Srivastav and Ponnani (2011). | Outward dimples | NACA 0018 | Numerical | - | Airfoil | A steady-state simulation was carried out under velocity 20 m/s, around an airfoil of span 0.8 cm at various AOA. Round shaped dimple performed better in minimizing the wake size, hence suitable for aerodynamic efficiency and stability. |
| 2. | Hossain et al. (2015) | In/outward dimples | NACA 4415 | Experimental | √ | Wing | Series of wind tunnel tests were carried out, and an inward dimple showed the best performance and has improved lift by 16.43% and degrades drag by 46.6%, at velocity 43 m/s. |
| 3. | Ali et al. (2017). | Sand grain | NACA 2412 | Numerical | √ | Wing | Steady-state CFD simulation was carried out at two different velocities and has proven the wing performance has sensitivity nature to roughness and also differs for compressible and incompressible flow. |
| 4. | Masud et al. (2017). | Outward dimple | NACA 2412 | Numerical | - | Wing | The sinusoidal wave LE with outward dimples shows better performance at stalling angle by increasing lift 18% and decreases drag by 20% compared to the baseline wing |
| 5. | Agarwal and Kumar (2016). | Vortex generators | NACA 4412 | Numerical | √ | Wing | Vortex generators have a high effect on aerodynamic efficiency at higher AOA and have a negative effect at low AOA; all these are controlled by the optimum positioning of VG on the wing surface. |
| 6. | Seshagiri et al. (2009). | Vortex generators | | Experimental | √ | Wing | Static vortex generators have shown 25% improvement in lift curve at 45 m/s and have shown diminished pressure drag with more considerable performance enhancement. |
| 7. | Jumahadi et al. (2018). | Vortex generators | NACA 4415 | Experimental | - | Wing | Active hybrid vortex generators have potential better performance at the sub-sonic condition with 11.3% improvement in lift and 16.5% increase in drag but decrease at high AOA. |
| 9. | Binci et al. (2017). | Inward dimple | NACA 64-014A | Both | √ | Wing | A dimple wing of 1.4m span is investigated under 40 m/s and with 0.3% turbulence intensity, resulted that about 2.81% C_D decreases and 2.93% for different turbulence model. |

Separation bubbles formed at the cavities vitalize flow transition and prolongs boundary layer separation. Thus, varying aspect ratio dimples investigated for efficient skin-friction drag and lift (Rajasai et al., 2015). From the researchers' work, it is clear that the flow over the cavity splits into two, one which circulates inside the cavity and the other passes over. Hence, enormous explorations are available, which may provide a solution for improving aerodynamic efficiency.

2.3.2 Behaviour of attached flow and re-attached flow

The boundary layer formation is due to two main factors, 1) pressure distribution and pressure variation over the airfoil and 2) shear stress distribution due to friction of airflow over the airfoil. Streamwise pressure generates and adverse pressure gradient decelerates the flow due to the counter-rotating shearing effects near the wall (Makwana and Makadiya, 2014). The general nomenclature of the airfoil is shown in Figure 2.2 (Makwana and Makadiya, 2014).

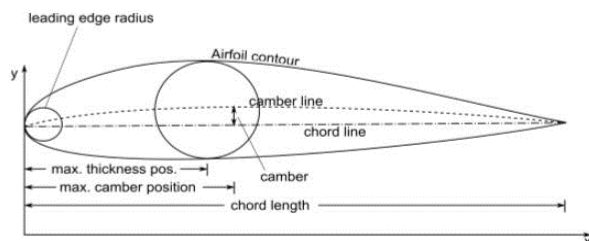


Figure 2.2 Airfoil nomenclature (Makwana and Makadiya, 2014)

A controlling study was carried out for the lift and drag using NACA 4412 airfoil (Carlson et al., 2004), with Mach number 0.1 at 8° AOA. At this moderate AOA, separation bubbles and periodic vortex shedding start to grow with a wake formation. Further increasing the AOA creates layered-up separation bubbles on the suction side with unsteady wake formation.

An experimental investigation of NACA 0012 airfoil has been carried out to study the dynamic feature of the wake formation of the airfoil at different AOA (Mehdi and Mehrdad, 2017). Tests were carried at 20 m/s with 5% turbulence intensity. Results indicated that beyond 0.5C and constant increase in AOA shifts the velocity profile negative, resulting in wake formation in the adjacent stations.

The low speed and low Re airfoil (such as NACA 2412) experiences the surface separation at 8° AOA (Hu and Yang, 2008), then transits to the turbulence layer with kelvin-Helmholtz unsteady vortex structure. This detached boundary layer re-attaches after turbulence transition along with a generation of laminar separation bubbles.

These bubbles degrade lift coefficient as in increasing AOA, resulting in an early stall due to the energized adverse pressure gradient. This energized pressure gradient generates a circulation effect with an active vortex (Ramprasad and Devanandh, 2015). These effect increases lift to a certain point along with the development of induced drag, which degrades further aerodynamic performance. Thus, the stalling point of NACA 2412 airfoil lies in the range of 14° to 16° AOA (Miller, 2012, Matsson et al., 2016).

Boundary layer detachment deals with the separation of the fluid flow from the solid surface. These separations are due to the rotation of flow with a leap in velocity components due to thickening of co-rotational flow. Dimples over the sphere (Choi et al., 2006) generate lesser drag due to the turbulent boundary layer formation because the momentum generated in the turbulent boundary layer is comparatively more significant than laminar boundary layer flow, thus delays the flow separation. Thus, surface roughness delays the boundary layer separation due to the energized and frictional behaviour of the fluid near the surface wall.

The performance of the airfoil/wing termed to serve better until the stalling condition beyond which the drag increases drastically. The stalling condition of the plain airfoil arises beyond 12° AOA (Chen et al., 2013); here, the accuracy prediction is difficult. At higher AOA the pressure drag increases leading to flow separation (Sagol et al., 2013). Drop-in pressure occurs due to laminar separation bubbles which temps the flow to detach from the surface (for smooth airfoil).

As in the case of the rough airfoil, the dropped down pressure gets re-energized due to the generation of linear momentum and re-circulation of the flow due to the trapped in air particles inside the cavity. These laminar separation bubbles have a governing role in altering the aerodynamic performance of an airfoil. The size of the laminar separation bubbles differs with Re_c ; the size get minimizes as the Re_c increases.

The viscous force around the airfoil increases with lower Re_c , which contributes much to boundary layer formation (Winslow et al., 2017). The flow does not show constant behaviour below $10^6 Re_c$. Cambered airfoil shows better performance with Re_c ranging around 10^5 (Winslow et al., 2017). As the AOA increases the boundary is more pronounced to the shear layer, resulting in transition of separation point towards LE. The transition of the flow takes place when the flow reaches the critical Re_c . Therefore, it is clear that the airfoil performance accompanied by boundary layer characteristics is very sensitive to Re_c ranges.

2.4 Dimple surface behaviour and its aerodynamic performance

The improvement in aerodynamic design and its sustainability in the aircraft industry had its leap right from 1903. Introducing dimples on to a smooth surface will recirculate the flow by the generation of swirling vortices and thus keeps the flow attached

for a longer period of time. Thereby, these re-attached flows will reduce the pressure drag formation with increasing the stalling characteristics (as shown in Figure 2.3). Critical R_e is induced at lower AOA as in the case of the dimpled surface compared to a smooth surface (Bearman and Harvey, 1976). At higher C_d regime of a smooth airfoil, the laminar flow over the surface changes at the point of maximum thickness. At this case, critical R_e takes place if the rough surface is used.

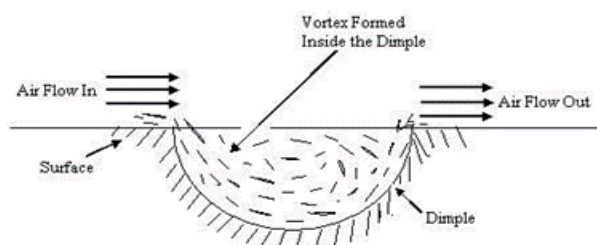


Figure 2.3 Diffusion of flow within the cavity (Kamath et al., 2016)

A summary of existing dimple variant and aerodynamic performance of variable shapes are tabulated in Table 2.2 and Table 2.3 below. Spherical dimples (Sobhani et al., 2017) placed at the pressure side of the NACA 0021 airfoil at 9 m/s, and 5% of turbulence shows better performance in generation of efficient flow. Indentation of a spherical dimple of $h/d = 0.1$ over a flat plate (Vincent and Mapple, 2006) has been studied to determine the vortex shedding due to the adverse pressure gradient at the boundary layer separation. Studies clearly states, at AOA the transition point is pulled near the LE (Sobhani et al., 2017, Vincent and Mapple, 2006, Robarge et al., 2004).

Recessed dimples showed up to be the potential passive modifier compared to VG, tabs and tripwires. Shallow dimple ($h/d \approx 1$) demonstrated better performance to reduce pressure losses by separated flows without added drag. The computational study on bumpy (protruded dimples) airfoil clearly showed that at 12° AOA the flow got separated for

smooth airfoil (Saraf et al., 2018), whereas the flow got re-attached for bumpy airfoil and remains same even at higher AOA. Therefore it is clear that these passive modifiers generate stable flow structure due to the generation of the streamwise vortex, which breaks the rolling-up vortices, thereby keeps the flow attached. The effect of suction bump (protruded dimple) over the suction surface of NACA 0012 (Yousefi and Saleh, 2015) wing were numerically studied. This study was based on optimizing the length of the suction jet. Upon analysing, the results show that increasing the length of the suction jet improves L/D by 43% and also delays the separation flow.

An array of dimples are punched near the LE of Tyrrell026 wing (Beves and Barber, 2017). Upon analysis, the baseline with endplate showed counter-rotating vortices with waviness propagating downstream, but the dimple wing model eliminates this waviness. The flow turbulence formation is boosted by placing a corner dimple or square dimple, thereby keeps the flow attached (Livya et al., 2015). Thus the indentation or cavities placed near the TE showed better performance (Vuddagiri et al., 2016, Wang et al., 2015).

Dimples create artificial vortices which delay boundary layer separation, and the effectiveness of the pressure distribution is stronger only up to 5 rows of dimples, according to the study (Ramprasad and Devanandh, 2015). This lag of pressure distribution is mainly due to the alternate interaction of the local vortices, which weakens the additional thrust. Increasing the depth of the dimple improves the aircraft climb and range (Miller, 2012) by the formation of the longer boundary layer at higher AOA and also experimentally proved that there is 18.3% enhancement in boundary layer compared to baseline wing.

Table 2.2 Existing dimple parameters


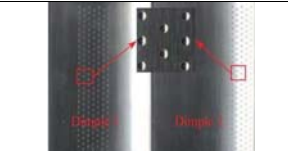
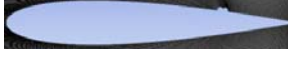
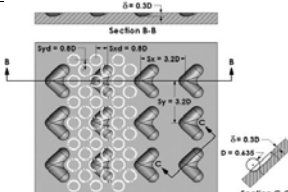
| References | Roughness shape | Airfoil | Diameter/width | Depth | Spacing | | Location | Figure | Highlights |
|--------------------------|-----------------|-----------|----------------|---------------------------------|---------------|-----------|----------------|--|--|
| | | | | | Stream wise | Span wise | | | |
| Saraf et al. (2017) | Semi-circular | NACA 0012 | 0.02 of chord | N/A | Single dimple | | 0.75C |  | The aerodynamic performance increases by 7% for lift and decreases by 3% for drag at this orientation. |
| Zhao et al. (2016) | Semi-circular | N/A | 1 mm | 0.2 mm | 5.2 mm | 3 mm | 0.30C to 0.60C |  | These orientations of the dimples performed better than 0.75C to 0.9C. |
| Saraf et al. (2018) | Irregular bump | NACA 0012 | 0.02C | Single bump (protruded dimples) | | | 0.75C |  | As the AOA increases, the flow separates and reattaches on to the bumpy surface. |
| Jordan and Wright (2011) | V-Shaped dimple | N/A | 0.635 cm | 0.3D | 3.2D | 3.2D | N/A |  | Three hemispherical dimples are interconnected to form V-shaped dimple. |

Table 2.2 Existing dimple parameters (continue...)



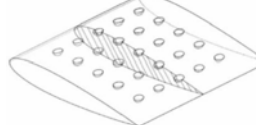

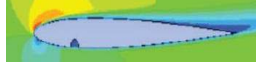

| References | Roughness shape | Airfoil | Diameter/width | Depth | Spacing | | Location | Figure | Highlights |
|--------------------------------|-------------------------|---------------|-----------------|----------|---------------|-----------|-----------------|--|--|
| | | | | | Stream wise | Span wise | | | |
| Sobhani et al. (2017) | Spherical dimple | NACA 0021 | 0.08C | 0.08C | Single dimple | | 25%C |  | This dimple is tested in a vertical axis wind turbine on pressure side, which showed better performance compared to the dimple at the suction side. |
| Ramprasad and Devanandh (2015) | Spherical dimple | SELIG 4083 | 5 mm | 0.5 mm | 8 mm | 10 mm | N/A |  | Low aspect ratio airfoil with high nonlinear lift curve is used in Mini Arial Vehicles, which resulted in improved flow behaviour. |
| Wang et al. (2015) | Semi ellipsoidal dimple | NACA 0018 | 5 mm/ 3.75 mm | N/A | 25 mm | 25 mm | Suction surface |  | Twenty-five dimples were textured over the wing, which reduces frictional force over the surface. This orientation recovers and reconnects the separated shear layer over the surface. |
| Vuddagiri et al. (2016) | Circular dimple | NACA 0018 | 33 mm | 15 mm | Single dimple | | 62%C |  | Smooth NACA 0018 airfoil stalls at 15° AOA, whereas airfoil with cavity stalls at 18° AOA. |
| Al-Obaidi and Pei Soh (2016) | Elliptical dimple | N/A | 0.04C/ 0.03125C | 0.025 C | Single dimple | | 20%C |  | At low-speed condition, the dimple at the pressure side shows a gradual increase in aerodynamic performance at all AOA. |
| D'Alessandro et al. (2019) | Spherical dimple | NACA 642-014A | 4.7%C | 0.705 %C | Single dimple | | 55%C |  | The dimples placed before or on the laminar separation bubble point shows improved aerodynamic characteristics and keeps the flow reattached. |

Table 2.3 Aerodynamic performance of different dimple shapes

| Reference | Airfoil type | Dimple shape | Mach No / velocity | R_e | Best result drawn | | | | |
|---------------------------------|--------------|---------------------|--------------------|-------------------|--------------------------|----------|----------------|-----------|------------------|
| | | | | | Max lift before stalling | Min drag | Stalling angle | (L/D) max | AOA at (L/D) max |
| Livya et al. (2015) | NACA 0018 | Square and compound | 30 & 60 m/s | N/A | 0.18 | 0.05 | 18° | 5.6 | 14° |
| Saraf et al. (2017) | NACA 0012 | Semi spherical | 7.3 m/s | N/A | 1.29 | -0.241 | 14° | 8.29 | 10° |
| Venkatesan et al. (2018) | NACA 2412 | Square | 30 m/s | N/A | 1.15 | 0.38 | 16° | N/A | N/A |
| Ramprasadh and Devanandh (2015) | SELIG 4083 | Sphere | 12 m/s | N/A | 1.40 | 0.02 | 24° | 6.04 | 4° |
| Chakroun et al. (2004) | NACA 0012 | Groove | 10 m/s | 1.5×10^5 | 0.9247 | 0.025 | 12° | 21.45 | 6° |
| Wang et al. (2015) | NACA 0018 | Semi ellipsoidal | 20 m/s | 3.2×10^5 | 0.17 | 0.03 | 15° | N/A | N/A |
| Al-Obaidi and Pei Soh (2016) | NACA 0012 | Elliptical dimple | 10 m/s | N/A | 0.82 | 0.022 | N/A | 18.49 | 5° |

The concept behind boundary layer separation was studied with the help of dimples on vehicle aerodynamics (Chear and DoI, 2015). The simulation was carried out over a surface with dimples of different dimple ratio of 0.05, 0.2, 0.3, 0.4 and 0.5. Upon analysis, for less than 40m/s, $K-\epsilon$ turbulence model with dimple ratio of 0.4 showed 1.95% of drag reduction compared to other orientation and plain surface.

2.5 Grooved surface behaviour and its aerodynamic performance

Net surface drag reduction along with the performance enhancement has been observed by intending grooves/ riblets over the flow surface (few existing groove parameters are listed in Table 2.4. Passive strategy study has been carried over the boat-tailed bluff body with counter transverse grooves over a R_e of 9.6×10^4 (Mariotti et al.,

2018). The flow over grooved surface project out significant delay of flow separation with productive 9.7% reduction in drag.

An experimental analysis was carried on NACA 0012 wing with wired roughness with R_e of 1.5×10^5 (Chakroun et al., 2004). From the study, it is proved that the smooth airfoil wing generates more significant lift and minimal drag compared to wired wing up to 10° AOA. Beyond that, increasing AOA increases the pressure gradient, drastically leads to stalling condition due to the movement of separation point towards the LE. The condition is because of the viscous stresses present within the boundary layer leading to high skin friction drag due to the presence of wired roughness.

As in the case of a smooth airfoil at 0° AOA, the laminar separation bubbles and turbulence flow transition are located at 0.59C & 0.71C, and flow reattaches at 0.77C. At 3° AOA separation point falls to 0.37C and reattaches at 0.54C. At 6° AOA the separation point falls to 0.40C, this shows almost the entire suction surface is filled with turbulence, and thus separation bubbles are not present.

Implementing a shock control bump (Mazaheri et al., 2015) on the wing surface has improved lift by 28%, L/D by 23% and degrades drag by 33%. The effectiveness of the boundary layer has been improved by deflection of steam-wise counter-rotating vortices. Longitudinal triangular grooves were intended over a non-dimensional flat plate in-order to study the heat transfer and drag characteristics. From Walsh and Weinstein (1979) study, it is clear that the flow becomes turbulent at $y^+ = 30$ for a base flat plate. Flow over the model varies from 15 m/s to 40 m/s, which shows a 4% to 5% reduction in drag characteristics in the case of V-groove type configuration.